EurJIC
European Journal of Inorganic Chemistry

Research Article
doi.org/10.1002/ejic.202300660

Chemistry Europe
European Chemical Societies Publishing

www.eurjic.org

Shedding Light on Eu(III) β-Diketonate Compounds with 1,2-Bis(diphenylphosphino)ethane Oxide Ligand: an Optical Study

Paulo R. S. Santos,[a] Ashley A. S. S. Jesus,[a] William B. Lima,[a] Joaldo G. Arruda,[a] Wagner M. Faustino,[a] Maria C. F. C. Felinto,[b] José R. Sabino,[c] Hermi F. Brito,[d] Israel F. Costa,[d] Renaldo T. Moura, Jr.,[e] Albano N. Carneiro Neto,[f] Oscar L. Malta,[g] Huayna Terraschke,[h] and Ercules E. S. Teotonio*[a]

A series of novel lanthanide β-diketonate coordination compounds containing the ancillary ligand bis(diphenylphosphino) oxide ($dppeO_2$) have been synthesized, characterized, and studied spectroscopically. The compounds of formulas $Ln(\beta\text{-dik})_3(dppeO_2)$, where Ln: Eu and Gd and β-dik ligands as tta (**Ln-1**), btf (**Ln-2**), bzac (**Ln-5**) and tfac (**Ln-4**), and $Ln_2(\beta\text{-dik})_6(dppeO_2)$ with ligand dbm (**Ln-3**) and fod (**Ln-6**). Their photophysical properties were investigated from the Judd-Ofelt intensity parameters (Ω_λ), radiative (A_{rad}) and non-radiative (A_{nrad}) rates, intrinsic (Q^{Eu}_{Eu}) and overall (Q^{L}_{Eu}) quantum yields, and CIE (x,y) color coordinates. The **Eu-5** and **Eu-6** compounds have the first excited triplet states T_1 (around 18802 and 18976 cm^{-1}, respectively) almost resonant with the Eu^{3+} $^5D_0$ emission level, whereas the complexes **Eu-1**, **Eu-2**, **Eu-3**, and **Eu-4** exhibited higher T_1 energies. The A_{rad} values were predominantly driven by the intensity parameter Ω_2, suggesting more pronounced angular changes in the first coordination sphere of the Eu^{3+} ion. The A_{nrad} values also exhibited significant changes with the β-diketonate ligands. **Eu-1** showed the highest value of Q^{L}_{Eu} (60%), indicating a more efficient intramolecular energy transfer process. On the other hand, **Eu-5** and **Eu-6** compounds showed Q^{L}_{Eu} values equal to 18.7% and 16.5%, respectively, which indicates the presence of luminescence quencher channels.

Introduction

In the coordination chemistry of trivalent lanthanide ions (Ln^{3+}), the ligand characteristics are essential to determine the chemical, structural, and spectroscopic properties of these compounds. Notably, organic ligands generally act as luminescence sensitizers for Ln^{3+} ions, overcoming the low molar absorptivity of the parity-forbidden intraconfigurational-4f transitions.[1] As a result, several highly luminescent complexes with β-diketonate and carboxylate ligands, particularly of the Eu^{3+} and Tb^{3+} ions, have been synthesized.[2a,b] Many of them have potential applications for optical sensing,[3a] light-emitting devices[3b,c] luminescent thermometers,[3d] optoelectronics,[3e] and theragnostic & bio-imaging.[3f,g]

Theoretical and experimental studies have revealed that the main intramolecular energy transfer channel in the sensitizing process involves the singlet (S_n, principally n = 1 and 2) and the low-lying triplet (T_1) excited states of the organic ligand as absorbers and energy donor, respectively.[4] Therefore, the relative T_1 state position and acceptor energy levels of the Ln^{3+}

[a] P. R. S. Santos, A. A. S. S. Jesus, W. B. Lima, J. G. Arruda, W. M. Faustino, E. E. S. Teotonio
Departamento de Química
Universidade Federal da Paraíba
58051-970, João Pessoa, PB (Brasil)
E-mail: teotonioees@quimica.ufpb.br

[b] M. C. F. C. Felinto
Instituto de Pesquisas Energéticas e Nucleares-IPEN/CNEN
São Paulo, SP, 05508-000 (Brasil)

[c] J. R. Sabino
Instituto de Física –
Universidade Federal de Goiás
74690-900, Goiânia, GO (Brasil)

[d] H. F. Brito, I. F. Costa
Instituto de Química
Universidade de São Paulo
05508-900, São Paulo, SP (Brasil)

[e] R. T. Moura, Jr.
Departmento de Química e Física
Universidade Federal da Paraíba
Areia, PB, 58397-000 (Brasil)

[f] A. N. Carneiro Neto
Physics Department and CICECO –
Aveiro Institute of Materials
University of Aveiro
Aveiro, 3810-193 (Portugal)

[g] O. L. Malta
Departamento de Química Fundamental
Universidade Federal de Pernambuco
Recife, PE-50740-560 (Brazil)

[h] H. Terraschke
Institute of Inorganic Chemistry
Christian-Albrechts-Universität zu Kiel
Max-Eyth-Str. 2
24118 Kiel (Germany)

Supporting information for this article is available on the WWW under https://doi.org/10.1002/ejic.202300660

Research Article
doi.org/10.1002/ejic.202300660

ions are the driving force for an efficient sensitization process. In particular, some β-diketonate ligands have presented energy structures in good resonance conditions to efficiently transfer energy to the $^5D_1$ and $^5D_0$ levels of the Eu^{3+} ion.[5] However, the positions of the excited T_1 states of these ligands can vary significantly with the structural properties of the complexes. In addition, ligand-to-metal charge transfer states (LMCT) of low-energies can also affect the luminescent properties of the lanthanide β-diketonate complexes.[6a,b]

The coordination chemistry of Ln^{3+} tris-β-diketonate complexes is not determined exclusively by a single type of ligand. Instead, additional neutral molecules are frequently used to interact with the metal center, leading to a more saturated chemical environment around the metal center. However, when such ligands have high-energy vibrational modes, efficient deactivation of the emitting level can occur by multi-phonon processes.[7] Among the ancillary ligands, water and alcohol molecules from the hydrated salt or the solvents play the most important role in luminescence quenching. To circumvent this detrimental effect, ligands with high charge donating capacity may be added to the reaction medium in a one-pot process, generally resulting in higher luminescence compounds.[8] An alternative strategy is to substitute the quencher molecules from precursor complexes in a later reaction step. Although this procedure is more costly, it provides a background for analyzing the role of the ancillary ligand in the optical properties of the metal center.

Trialkylphosphine oxides have been intensively investigated as ancillary ligands for the lanthanide β-diketonate complexes. As the P=O bonds are highly polarized, these ligands can form significantly stronger bonds with different classes of metal ions. Therefore, it is not surprising that trialkylphosphine oxides easily replace water or alcohol molecules in the first coordination sphere. Consequently, the chemistry of coordination compounds involving the monodentate ligands R_3PO, where R: CH_3 (methyl), CH_2CH_3 (ethyl), C_6H_{12} (cyclohexyl), or C_6H_6 (phenyl), has been extensively investigated.[9a,b] In this case, mononuclear species have been obtained, in which the steric hindrances of the substituent R groups play a central role in defining the stoichiometry and structural properties of the complexes. It is worth mentioning that different classes of lanthanide β-diketonate complexes with R_3PO ligands showing anomalous luminescent properties have been reported.[10a,b]

Multidentate bis and tris(alkylphosphine) oxides ligands containing aliphatic and aromatic spacer groups have been the subject of intensive studies due to the possibility of forming mononuclear, binuclear complexes, or coordination polymers.[11] Recently, our research group also carried out a systematic study on new highly luminescent Eu^{3+} tris-β-diketonate complexes containing organometallic units[12] In addition, Hasegawa and co-workers[13a–e] investigated a series of compounds containing diphenylphosphine oxide derivative ligands as ancillary bidentate ligands, which make a bridge between two tris(hexafluoroacetonate)lanthanide(III) and tris(dipivaloylmethanate)lanthanide(III) complexes. Further, the spectroscopic behavior of the ligand-metal charge transfer (LMCT) state has also been reported.[14a–c] Recently, Tb^{3+}-Eu^{3+} mixed coordination polymers containing hexafluoroacetonate and $dppeO_2$ were synthesized, and their structural properties were also investigated.[14d–e]

Despite the advances of this class of lanthanide complexes containing ligands derived from bis(diphenylphosphino) oxide, studies reporting on the luminescent properties of compounds with different β-diketonates are very scarce in the literature. So far, to the best of our knowledge, only two works have reported on compounds of lanthanide ions focusing on complexes with bis(diphenylphosphino) oxide with aliphatic spacer. For example, 1D coordination polymer $\{Sm(hfac)_3(L1)\}_\infty$ (where L1 and hfac stand for 1,4-bis(diphenylphosphino)butane oxide and hexafluoroacetylacetonato, respectively) exhibiting high orange emission were reported by Xu et al.[15]

Herein, we report a systematic study on the syntheses and photophysical properties of highly luminescent Eu^{3+} and Gd^{3+} compounds containing bis(diphenylphosphino)ethane oxide ($dppeO_2$) and different β-diketonate (β-dik) ligands, where β-dik: thenoyltrifluoroacetonate (tta), benzoyltrifluoroacetonate (btf), dibenzoylmethanate (dbm), 2-trifluoroacetonate (tfac), benzoylacetonate (bzac), and 2,2-dimethyl-6,6,7,7,8,8,8-heptafluoro-3,5-octanedione (fod) (Figure 1). To better understand the spectroscopic properties of these compounds, various techniques were used, including diffuse reflectance, excitation, and emission spectra, as well as luminescent decay curves. For the Eu^{3+}

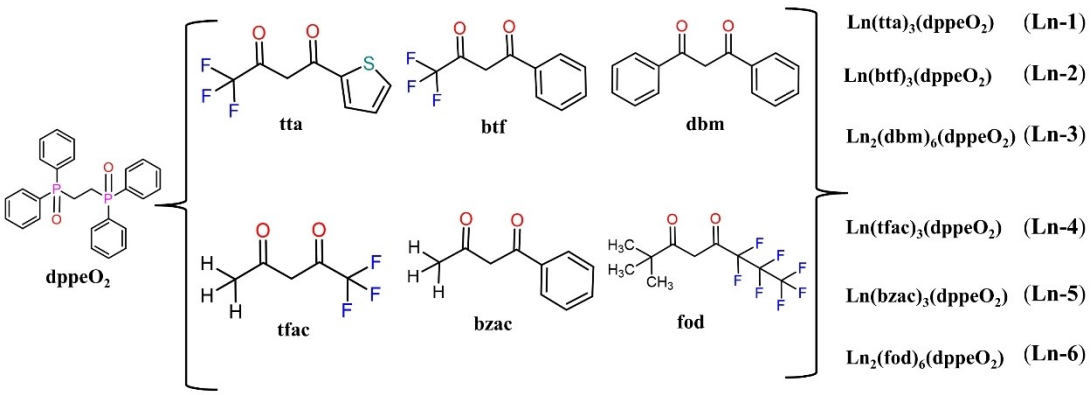

Figure 1. Structural formulas of ancillary $dppeO_2$ and β-diketonate ligands.

Research Article
doi.org/10.1002/ejic.202300660

-based compounds, a quantitative investigation was carried out from Einstein's spontaneous emission coefficients ($A_{0\rightarrow J}$), Judd-Ofelt intensity parameters (Ω_λ, where $\lambda = 2$ and 4), intrinsic (Q^{Eu}_{Eu}) and absolute (Q^{L}_{Eu}) quantum yields.

Results and Discussion

Infrared spectrum analysis

In general, the synthesized coordination compounds are moderately soluble in ethanol and methanol and insoluble in other common organic solvents such as acetone, acetonitrile, dichloroethane, and chloroform. In addition, elemental analysis data for the synthesized samples are in good agreement with the following proposed formulas Eu(β-dik)$_3$(dppeO$_2$), except for the complex with dbm and fod ligands, which their data agree with the formula Eu$_2$(β-dik)$_6$(dppeO$_2$). It is important to note that these general formulas were also presented for polymeric [Eu(hfa)$_3$(dppeO$_2$)][14b] and dimeric [Dy$_2$(dpm)$_6$(dppeO$_2$)][16] compounds with the dppeO$_2$ ligand.

Fourier-transform infrared spectroscopy (FTIR) spectra of the Ln(β-dik)$_3$(dppeO$_2$) and Ln$_2$(β-dik)$_6$(dppeO$_2$) coordination compounds are shown in Figure S1. By comparing with those absorption spectra for their respective precursor aquo-complexes Ln(β-dik)$_3$(H$_2$O), the broad band around 3300 cm^{-1} due to the stretching assigned ν(O–H) vibrational modes of water molecules is not observed. This finding suggests that the ancillary dppeO$_2$ ligand has effectively replaced the water molecules in the first coordination sphere. Furthermore, the strong bands at around 1614 and 1578 cm^{-1} attributed to the ν(C=C) and ν(C=O) stretching modes are presented. With anomalous behavior, the complex **Eu-6** exhibited displacement of the bands attributed to the vibrational stretching modes ν(C=O) and the mixture of ν(C=C) and ν(C=O) from 1600 to 1622 cm^{-1}.[17] This phenomenon can be attributed to the great difference in the nature of the substituent groups, namely, a donating group (tert-but) and a strongly electron-withdrawing group containing seven fluorine atoms that by inductive effect should contribute to the shortening of the C=O bond. Therefore, this result is a strong indication that the coordination of β-diketonates ligands to the lanthanide ion occurs in a bidentate chelating manner through oxygen atoms.[10a] Strong absorption bands appearing between 1139–1159 cm^{-1} correspond to the P=O stretching mode. These results suggest that the complexes were obtained in their anhydrous form, where the H$_2$O molecules were replaced by the bis(phosphinoxide) dppeO$_2$ ligand molecules.

Single crystal X-ray crystallography

The structure of the polymeric compound **Eu-5** was resolved by X-ray analysis using the single-crystal method. According to structural data, this compound is characterized by a 1D coordination polymer chain along the a-axis, in which the dppeO$_2$ acts as a bridging ligand (Figure 2a). In addition, this system crystallizes in the monoclinic space group P2$_1$/c with a value of Z = 4 and a cell volume of 4928.5 Å^3. The octacoordinated unit EuO$_8$ contains six oxygen atoms from three bidentate chelating bzac ligands (O3A, O3B, O4A, O4B, O5A and O5B), and two oxygen atoms (O1 and O2) from two dppeO$_2$ bridging ligands.

It is interesting to point out that the phenyl substituent group in each bzac ligand is almost coplanar to the chelate ring. This arrangement results of the steric hindrance among these regions of bzac ligands and the substituent groups of the phosphinoxide ligands, resulting in a stronger interaction of the carbonyl oxygen atom with the lanthanide ion. On the other hand, Eu–O interactions involving oxygen atoms from carbonyl group containing CH$_3$ as substituent groups are longer ones. In fact, all bzac ligands are coordinated to the Eu^{3+} ion in asymmetry fashions, presenting different Eu–O bond distances (Table 1). This difference is more pronounced for the Eu–O5A and Eu^{3+}-O5B that have bond lengths equals to 2.437 and 2.326 Å, respectively. As can be observed in Figure 2a, two bzac molecules have their phenyl substituent groups close to phenyl moieties from dppeO$_2$ bridging ligands, resulting in a strong steric hindrance among them. This asymmetry is a consequence of the steric effects caused by the three β-diketonate ligands (Figure 2b). On the other hand, the smallest difference in bond lengths is found for the bzac ligand that has its chelating ring in the same plane as the Eu–O=P bonds. A similar behavior is observed for the Eu–O1=P and Eu–O2=P that present bond distances of 2.403 Å and 2.389 Å, respectively.

The SHAPE software was used to obtain information about the geometry of the coordination polyhedron, which calculates the continuously measured parameter (CShM) that is close to zero for the perfect polyhedron (Table S1). In the case of the complex [Eu(bzac)$_3$(dppeO$_2$)]$_\infty$, the lowest CShM value (0.924) was obtained for the triangular dodecahedron (point group D$_2$d) (Figure 2c). However, similar Eu(tfaa)$_3$(dppeO$_2$)]$_\infty$ com-

Table 1. Bond lengths/Å and angles/° for [Eu(bzac)$_3$(dppeO$_2$)]$_\infty$.

Bond lengths/Å		**Bond lengths/Å**	
Eu(1)–O(5A)	2.326(3)	Eu(1)–O(3A)	2.404(3)
Eu(1)–O(4B)	2.364(3)	Eu(1)–O(3B)	2.424(3)
Eu(1)–O(2)	2.389(3)	Eu(1)–O(5B)	2.437(3)
Eu(1)–O(1)	2.403(3)	Eu(1)–O(4A)	2.447(3)
Angles/°		**Angles/°**	
O(5A)–Eu(1)–O(4B)	147.46(10)	O(5A)–Eu(1)–O(3B)	75.84(10)
O(5A)–Eu(1)–O(2)	87.67(10)	O(4B)–Eu(1)–O(3B)	81.16(10)
O(4B)–Eu(1)–O(2)	105.93(10)	O(2)–Eu(1)–O(3B)	70.20(9)
O(5A)–Eu(1)–O(1)	96.23(10)	O(1)–Eu(1)–O(3B)	143.66(9)
O(4B)–Eu(1)–O(1)	88.77(10)	O(3A)–Eu(1)–O(3B)	70.75(9)
O(2)–Eu(1)–O(1)	145.80(9)	O(5A)–Eu(1)–O(5B)	70.91(10)
O(5A)–Eu(1)–O(3A)	77.15(11)	O(4B)–Eu(1)–O(5B)	140.36(9)
O(4B)–Eu(1)–O(3A)	73.67(10)	O(2)–Eu(1)–O(5B)	76.85(9)
O(2)–Eu(1)–O(3A)	140.47(9)	O(1)–Eu(1)–O(5B)	72.51(9)
O(1)–Eu(1)–O(3A)	72.91(9)	O(3A)–Eu(1)–O(5B)	129.19(10)

Research Article
doi.org/10.1002/ejic.202300660

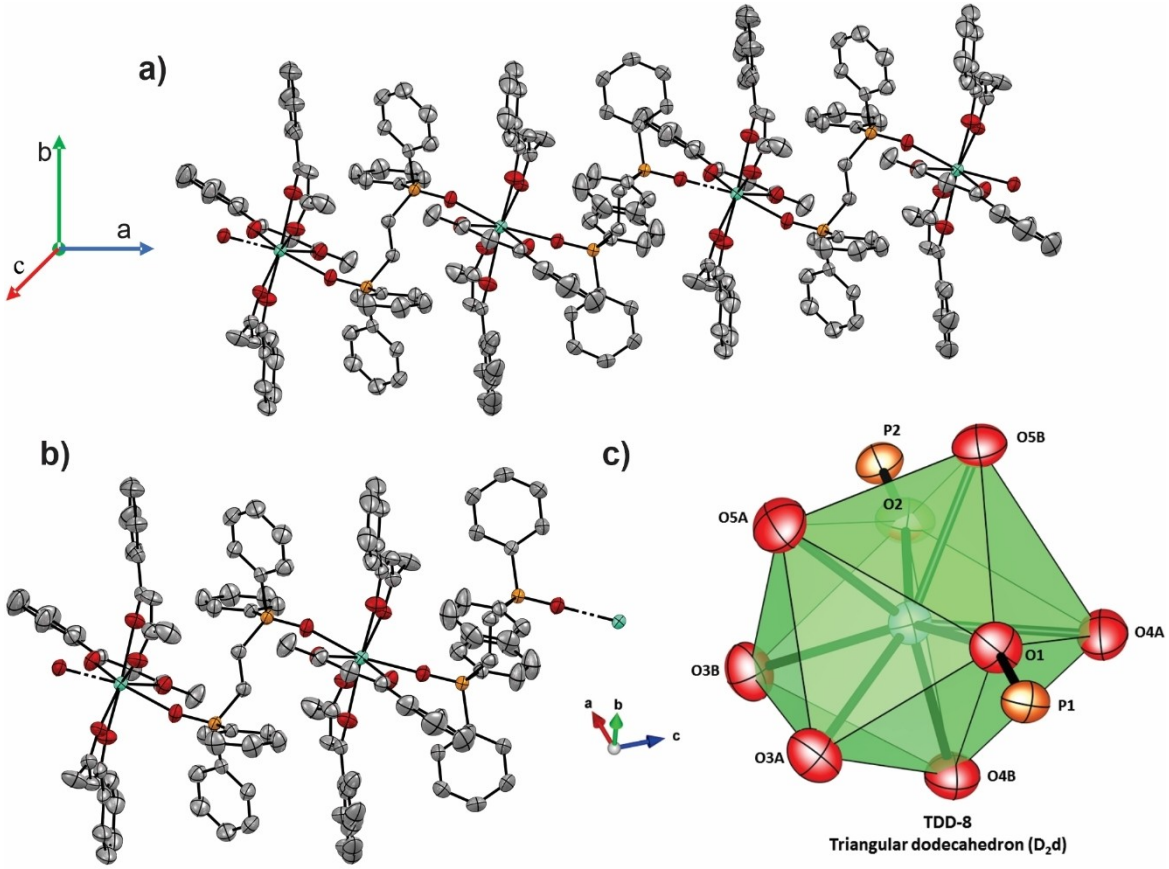

Figure 2. a) Structure of the complex $[Eu(bzac)_3(dppeO_2)]_\infty$ (hydrogen atoms have been omitted) ORTEP drawing (50% probability) along c axis. b) Asymmetric unit of the $[Eu(bzac)_3(dppeO_2)]_\infty$ coordination polymer c) Coordination polyhedron of the $[Eu(bzac)_3(dppeO_2)]_\infty$ ORTEP (50% probability). Carbon (gray), oxygen (red), europium (orange), nitrogen (blue), and hydrogen (white).

pounds exhibited a CShM value of 0.490 and a geometry close to a square antiprism of point group D_4d[14b] This difference in CShM fit can be explained by steric factors caused by the bzac ligand being larger than the tfaa ligand, which would lead to a stronger distortion of the coordination polyhedron of the complex with bzac. It is worth mentioning that the experimental PXRD pattern for Eu-5 (Figure S2) agrees with the simulated one, indicating its phase purity.

Thermal analyses

The thermal properties of the $Ln(\beta\text{-dik})_3(dppeO_2)$, where β-dik: tta (**Eu-1**), btf (**Eu-2**), bzac (**Eu-5**) and tfac (**Eu-4**), and $Ln_2(\beta\text{-dik})_6(dppeO_2)$ for β-dik: dbm (**Eu-3**) and fod (**Eu-6**) coordination compounds in the temperature interval from 25 to 900 °C were investigated based on the thermogravimetric (TGA) and differential thermal (DTA) analyses. As observed in Figure S3, no weight loss event occurs up to 270 °C in TGA curves of the compounds, which also reinforces their anhydrous character and high purity degrees. These results agree well with the FTIR and elemental analysis data. Most of the $Ln(\beta\text{-dik})_3(dppeO_2)$ compounds, except **Eu-3**, undergo a melting process just before the thermal decomposition, characterized by an endothermic peak above 240 °C. As noted in DTA curves (Figure S3a), the anhydrous **Eu-6** compound melts at a lower temperature, 120 °C. The extraordinarily high thermal stability of these solid compounds is likely owing to their structural rigidity. It is worth mentioning that their respective mononuclear complexes with triphenylphosphine oxide (tppo) ligand generally melt at lower temperatures.[2b] According to TGA/DTA curves, after the melting process, all compounds present two consecutive weight loss events up to approximately 700 °C. Although the anhydrous $Ln_2(fod)_6(dppeO_2)$ melts at a lower temperature, its thermal decomposition also begins around 300 °C. It is interesting to point out that the first thermal decomposition event in the TGA curves of these anhydrous compounds is the most pronounced one. In particular, it corresponds to almost 90% of the initial mass of the **Eu-6** compound. Based on these results, we can infer that the evaporation of the compounds probably accompanies their thermal decomposition processes. This finding aligns with the lower amount of the final thermal decomposition product expected of the lanthanide oxide (Ln_2O_3).

Research Article
doi.org/10.1002/ejic.202300660

Ligand excited states and luminescence spectra

Figure 3 shows the diffuse reflectance spectra of the Ln(tta)$_3$(dppeO$_2$) (**Eu-1** and **Gd-1)** and Ln$_2$(fod)$_6$(dppeO$_2$) (**Eu-6** and **Gd-6**) solid-state compounds recorded in the range from 250 to 500 nm. The diffuse reflectance spectra for Eu^{3+} and Gd^{3+} compounds (**Eu-2** and **Gd-2)**, bzac (**Eu-5** and **Gd-5)**, (**Eu-4** and **Gd-4**), (**Eu-3** and **Gd-3)** are shown in Figure S4. In general, these spectra exhibit broad absorption bands in the spectral 250–450 nm interval that may be assigned to intraligand $S_0 \rightarrow S_2$ and $S_0 \rightarrow S_1$ electronic transition (Figure 3), which present a strong π–π^* character. No narrow band from the intraconfigurational-4f^6 transition of the Eu^{3+} ion has been observed owing to the prominent intensities of ligand absorption bands. It is noteworthy that respective Eu^{3+} and Gd^{3+}-compounds exhibit quite similar spectral profiles, suggesting that only slight changes in the ligand electronic structures occurred by changing the lanthanide ion. Furthermore, the positions of these absorption bands are almost unchanged when compared to those of their respective tris-β-diketonate complexes.[11] In this work, the energy of the low-lying excited singlet state for each complex, S_1, was taken as the energy corresponding to the maximum absorbance of the band at the longest wavelength.

Although the similarity between the reflectance spectra of the Eu^{3+} and Gd^{3+} compounds is quite evident, the diffuse reflectance spectrum for Eu$_2$(fod)$_6$(dppeO$_2$) (**Eu-6**) compound presents an additional shoulder in the region of longer wavelength. This additional band may be attributed to a ligand-to-metal charge transfer (LMCT) transition ($S_0 \rightarrow$LMCT). The energy of this excited state (~26667 cm^{-1}) was determined from the deconvoluted absorption spectrum. This difference stems from the presence of an LMCT state almost resonant with the excited S_1 ligand state. As previously reported by Faustino e co-workers,[18] LMCT state with energy in the range of 20000 to 25000 cm^{-1} may play a key role in Eu^{3+} luminescence quenching, decreasing the population of the metallic center emitting state. In addition, the LMCT state can damage the antenna effect by deactivating either the low-lying singlet or triplet excited states, as reported in references.[12,17] Although the factors that result in low-energy charge transfer states in lanthanide ion complexes are still unclear in the literature, Eu^{3+}-compounds with diketonate ligands containing the tert-butyl group generally present LMCT of very low energy likely due to their high electron-donor capability, as reported in our previous manuscript.[10b]

The phosphorescence spectra of Gd^{3+}-complexes have been extensively used to mimic the electronic structure of the organic ligand in analogous systems containing Eu^{3+} ions (Figure S5). It is worth mentioning that Eu^{3+} and Gd^{3+} compounds with the same ligands generally present very similar structural geometries. In addition, it should be noted that the first $^6P_{7/2}$ excited state of Gd^{3+} ion is situated at ~32000 cm^{-1}. This energy level is comparatively high, and as a result, it is improbable to engage in the ligand-to-metal energy transfer process.[19]

To identify the T_1 state, the time-resolved phosphorescence spectra of the Gd^{3+} compounds were recorded at low-temperature (77 K) in the 430–700 nm range under excitation at 350 nm with a 1 ms delay time (Figure S5). This procedure eliminated contributions from the fluorescence band ($S_1 \rightarrow S_0$), which may overlap with the phosphorescence band ($T \rightarrow S_0$). The similar spectral profiles and positions of the phosphorescence bands to those of other complexes with the same β-diketonate ligands[12] suggest that dppeO$_2$ plays only a minor role in the excited states of these compounds. We applied the Jacobian transform to reflectance (Figure S6) and phosphorescence spectra (Figure S7) to convert the data to a more convenient scale (cm^{-1}). Thus, we used a Python code (see section **4**. in the Supporting Information).

The barycenter values of the phosphorescence bands (Table 2) of all compounds suggest that bzac (**Gd-5**) and fod (**Gd-6**) ligands exhibit lower energies of the T_1 state (18802 and 18976 cm^{-1}, respectively). Although these T_1 states are located at higher energies than the $^5D_0$ (ca. 17300 cm^{-1}) level, they are

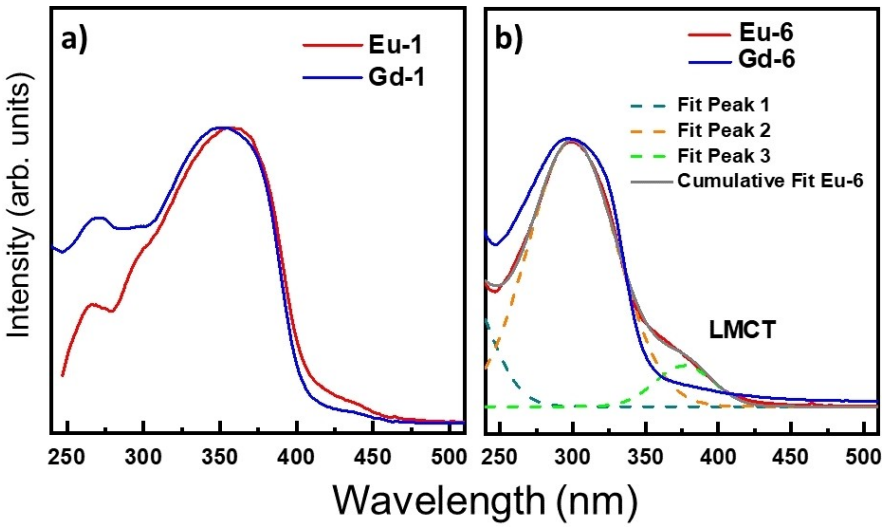

Figure 3. Reflectance spectra of the compounds in the solid state: a) Ln(tta)$_3$(dppeO$_2$) (**Eu-1** and **Gd-1)** and b) Ln$_2$(fod)$_6$(dppeO$_2$) (**Eu-6** and **Gd-6**).

Research Article
doi.org/10.1002/ejic.202300660

Table 2. Gd^{3+}-based compounds and their energies of the S_1 and T_1 excited states (in cm^{-1}).

Compound	Label	S_1	T_1
$Gd(tta)_3(dppeO_2)$	Gd-1	29107	19773
$Gd(btf)_3(dppeO_2)$	Gd-2	30872	19348
$Gd_2(dbm)_6(dppeO_2)$	Gd-3	28322	19970
$Gd(tfac)_3(dppeO_2)$	Gd-4	34332	19997
$Gd(bzac)_3(dppeO_2)$	Gd-5	30369	18802
$Gd_2(fod)_6(dppeO_2)$	Gd-6	34103	18976

slightly lower than the $^5D_1$ (ca. 19000 cm^{-1}) level of the Eu^{3+} ions. This energetic position (between $^5D_0$ and $^5D_1$ levels) does not favor the ligand-to-Eu^{3+} energy transfer but favors the backward energy transfer from the Eu^{3+}-to-ligand, leading to low absolute quantum yields, Q^L_{Eu} (e.g. the ratio between emitted and absorbed photons by the system) for **Eu-5** and **Eu-6** complexes. On the other hand, the T_1 states for other investigated compounds (Table 2) have barycenter energies higher than 19300 cm^{-1}, enabling more efficient $T_1 \rightarrow {}^5D_{0,1}$ energy transfer pathways.

Figure 4 depicts the excitation spectra of the Eu(β-dik)$_3$(dppeO$_2$) (β-dik: tta, btf, bzac and tfac) and Eu$_2$(β-dik)$_6$(dppeO$_2$) (β-dik: dbm and fod) coordination compounds in the spectral range from 250 to 580 nm. These spectra were recorded at 298 and 77 K temperatures, upon emission monitored at the $^5D_0 \rightarrow {}^7F_2$ transition of the Eu^{3+} ion (around 612 nm). All excitation spectra exhibit intense broad bands arising from $S_0 \rightarrow S_2$ and $S_0 \rightarrow S_1$ transitions. Besides, it is observed some narrow excitation bands attributed to the transitions: $^7F_0 \rightarrow {}^5L_6$ (393 nm), $^7F_{0,1} \rightarrow {}^5D_2$ (463 nm), $^7F_0 \rightarrow {}^5D_1$ (525 nm), and $^7F_1 \rightarrow {}^5D_1$ (534 nm) of the Eu^{3+} ion.[19]

The excitation spectra (Figure 4) reveal that the relative intensities of the ligand transitions may change significantly as a result of replacing β-diketonate ligand in the europium compounds, according to the following trend: **Eu-1** > **Eu-2**~**Eu-4** > **Eu-3**~**Eu-5** > **Eu-6**. Thus, qualitatively, a parallel can be drawn between this trend and the intrinsic (Q^{Eu}_{Eu}) and overall (Q^L_{Eu}) quantum yields in the luminescence sensitization mechanism of the Eu^{3+} ion in these compounds. The **Eu-1** compound exhibits the highest relative intensity, suggesting that it is the highest brightness among the investigated materials, as a consequence of the most efficient energy transfer from ligands to the Eu^{3+} ion in the Eu(tta)$_3$(dppeO$_2$) complex. On the other hand, the lowest luminescent sensitization efficiency can be attributed to the **Eu-6** compound because the relative intensities of both intraligand broad bands and $^7F_0 \rightarrow {}^5L_6$ (~394 nm) are significantly lower than that one from the

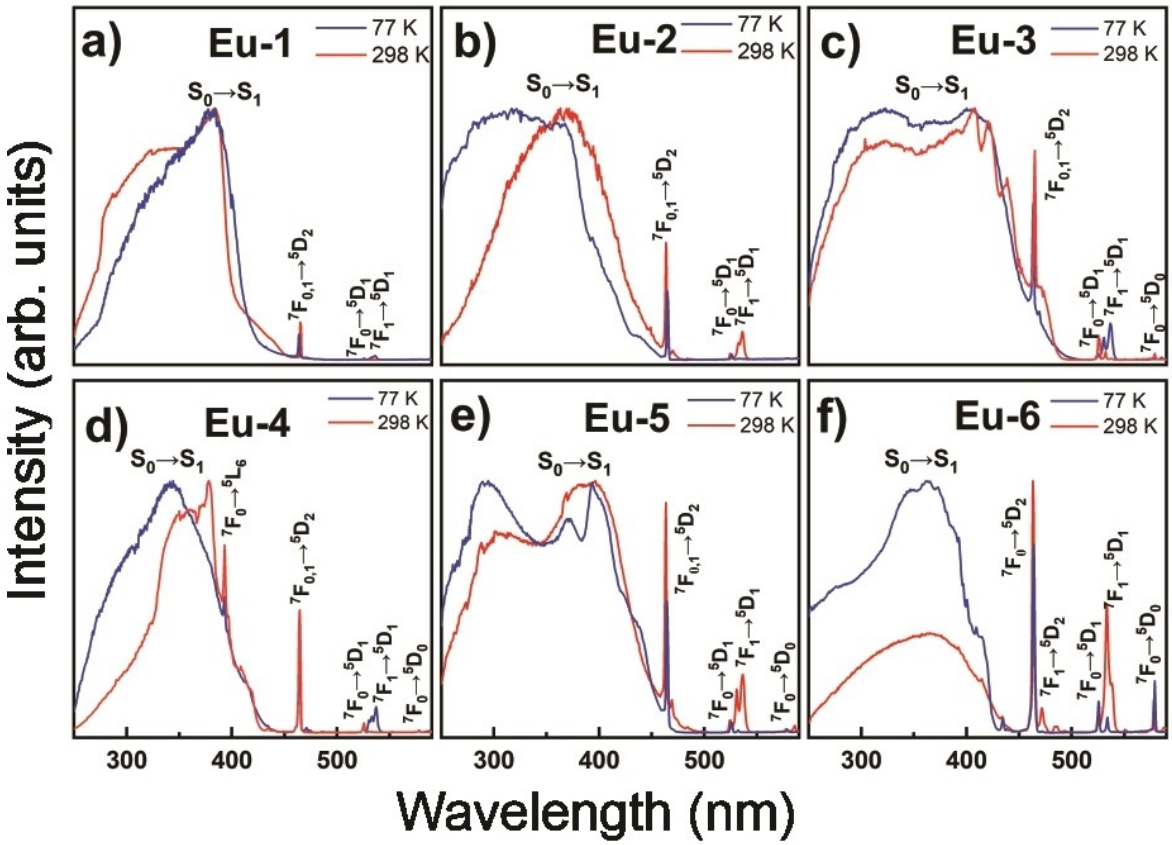

Figure 4. Excitation spectra of the Eu(β-dik)$_3$(dppeO$_2$) (**Eu-1**, **Eu-2**, **Eu-3**, and **Eu-4** when β-dik: tta, btf, dbm, and tfac, respectively) and Eu$_2$(β-dik)$_6$(dppeO$_2$) (**Eu-5** and **Eu-6** when β-dik: bzac and fod, respectively) coordination compounds recorded at 298 and 77 K temperatures with emission monitored at the intraconfigurational $^5D_0 \rightarrow {}^7F_2$ transition of the Eu^{3+} ion (ca. 612 nm).

Research Article
doi.org/10.1002/ejic.202300660

$^7F_0 \rightarrow {}^5D_2$ (~464 nm) transition as can be noted in the excitation spectrum at 298 K (Figure 4f). More interestingly, there is a significant increase in the relative intensity of the $S_0 \rightarrow S_1$ transition by decreasing the temperature. This result is in line with the diffuse reflection data (Figure 3 and S4), which indicates the presence of an LMCT state with energy at 26667 cm^{-1} for the **Eu-6** compound. Consequently, upon indirect excitation, the low-lying singlet and triplet excited states of the fod ligand may be significantly depopulated, leading to a less efficient luminescent sensitization in its compound. However, this quenching process is greatly minimized at a lower temperature. Furthermore, for the excitation spectra recorded at low temperature (77 K), it is also observed a decrease in the intensity of the broadband at around 270 nm. This result suggests that the luminescence sensitization of the Eu^{3+} ion at lower temperatures is more efficient upon an indirect excitation on the intraligand ($S_0 \rightarrow S_1$ transition). A significant decrease in the intensities of the intraconfigurational $^7F_0 \rightarrow {}^5D_2$ (464 nm) and $^7F_1 \rightarrow {}^5D_1$ (534 nm) transitions because of the decrease in the population of this level $^7F_1$ level is also shown. Other minor alterations in the spectral profiles are due to the decrease in the vibronic couplings with temperature. Apart from these spectral changes, the relative excitation intensities of the other transitions are less influenced by the lowering of temperature at 77 K.

The weaker relative intensities of the intraligand transitions in the excitation spectrum of the **Eu-5** compound (Figure 4e) may be associated with the very low energy of the triplet state, as will be discussed quantitatively later. Although no significant difference between the DRS spectra for other [Ln-(bzac)$_3$(dppeO$_2$)]$_\infty$ compounds has been observed, this also does not exclude the possibility of bands due to LMCT states are overlapped with those attributed to intraligand transitions. It is worth mentioning that LMCT states are common in complexes with bzac and dbm β-diketonate ligands,[20] which may also explain the low relative intensity of the $S_0 \rightarrow S_1$ transition observed for the **Eu-3** (Figure 4c).

The emission spectra of the Eu(β-dik)$_3$(dppeO$_2$) (β-dik: tta, btf, bzac and tfac) and Eu$_2$(β-dik)$_6$(dppeO$_2$) (β-dik: dbm and fod) compounds (Figure 5) in the range from 580 to 700 nm, recorded at liquid nitrogen temperature (77 K), are only composed by the typical narrow emission bands assigned to the $^5D_0 \rightarrow {}^7F_0$ (~578 nm), $^5D_0 \rightarrow {}^7F_1$ (~590 nm), $^5D_0 \rightarrow {}^7F_2$ (~612 nm), $^5D_0 \rightarrow {}^7F_3$ (~530 nm), and $^5D_0 \rightarrow {}^7F_4$ (~700 nm), being that one from the $^5D_0 \rightarrow {}^7F_2$ transition (~612 nm) as the most prominent. The emission spectra recorded at room temperature (~298 K) are also presented in Figure S8. Compared to the emission spectra for the Gd^{3+} compounds, the absence of the broad phosphorescence band from the coordinated β-diketonate ligands indicates that the energy transfer is efficient from the organic ligand to the lanthanide. Based on the reflectance and excitation data (Figure 3, Figure S4 and Figure 4), this intramolecular energy transfer process plays the most crucial role in the luminescent properties of the Ln(β-dik)$_3$(dppeO$_2$) (β-dik: tta,

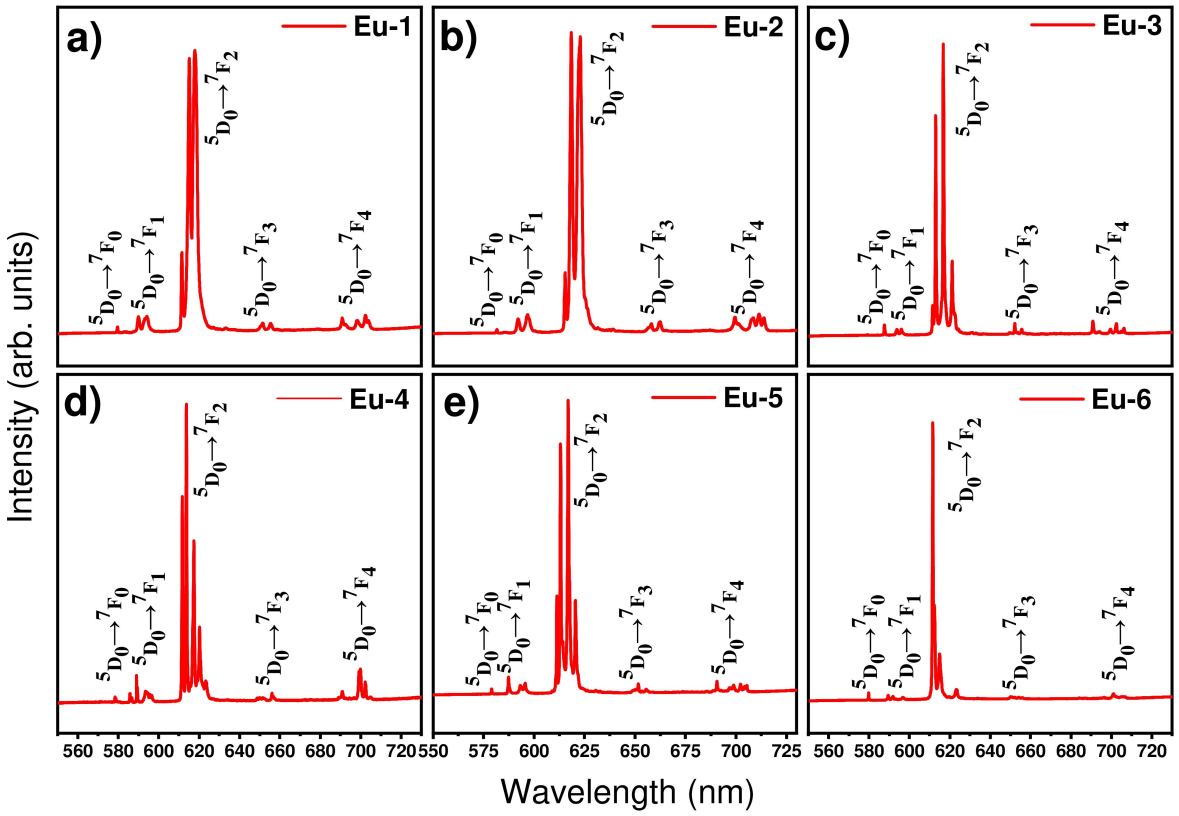

Figure 5. Emission spectra of the Eu(β-dik)$_3$(dppeO$_2$) (**Eu-1**, **Eu-2**, **Eu-5**, and **Eu-4** when β-dik: tta, btf, dbm, and tfac, respectively) and Eu$_2$(β-dik)$_6$(dppeO$_2$) (**Eu-3** and **Eu-6** when β-dik: bzac and fod, respectively) coordination compounds recorded at 77 K under excitation at 370 nm.

Research Article
doi.org/10.1002/ejic.202300660

btf, bzac, and tfac). However, a lack of phosphorescence and inefficient intramolecular energy transfer can also occur when S_1 and T_1 ligand states in the Eu^{3+} compounds are effectively quenched via LMCT states. This phenomenon is probably the critical factor in explaining the spectroscopic behavior of the $Ln_2(fod)_6(dppeO_2)$ compound.

Interestingly, the emission spectra for **Eu-1** and **Eu-2** compounds display similar profiles, suggesting that the chemical environments of the Eu^{3+} ions have very comparable symmetry. The same behavior is also observed when comparing the spectral data for **Eu-4** and **Eu-5** compounds. On the other hand, **Eu-3** and **Eu-6** show more distinct spectral profiles. In general, the bands due to the $^5D_0 \rightarrow {}^7F_J$ transitions split at the maximum of $(2J+1)$-components, indicating a single chemical environment around the Eu^{3+} ion. In particular, the presence of a single weak band due to the $^5D_0 \rightarrow {}^7F_0$ (579 nm) transition observed in all emission spectra agrees with this hypothesis. Even though the $dppeO_2$ ancillary ligand is probably coordinated in bridging mode, leading to binuclear or polymeric coordination compounds similar to that showed for complexes with hfa,[11] in which the Eu^{3+} ions are symmetrically equivalent. These spectral profiles align with the selection rules in J total angular number and symmetry, suggesting that the chemical environment around the Eu^{3+} ion belongs to the C_n or C_{nv} group point symmetry.[21]

The decay kinetics of the $^5D_0$ emitting level for the Eu(β-dik)$_3$($dppeO_2$) (β-dik: tta, btf, dbm and tfac) and $Eu_2(fod)_6(dppeO_2)$ compounds were analyzed from the luminescence decay curves (Figure S9), which were recorded with excitation and emission monitored at the intraligand ($S_0 \rightarrow S_1$) and Eu^{3+} ion ($^5D_0 \rightarrow {}^7F_2$) transitions, respectively. These curves were best fitted to a single exponential, reinforcing the emission spectra profiles that indicate a presence of only a single chemical environment for the Eu^{3+} ion in the investigated compounds. It is important to mention that the luminescence decay lifetime (τ) of $^5D_0$ level was obtained from $I(t) = I(0)e^{-t/\tau}$. The τ values have contributions of radiative (A_{rad}) and non-radiative (A_{nrad}) rates, according to Equation 1:

$$\tau = \frac{1}{A_{rad} + A_{nrad}} = \frac{1}{A_{total}} \quad (1)$$

With the emission spectra and luminescence lifetime decay data, we also evaluated quantitatively the photoluminescent properties of the synthesized compounds based on Einstein's spontaneous emission coefficients ($A_{0\rightarrow J}$), Judd-Ofelt intensity parameters Ω_λ (λ = 2 and 4), and intrinsic quantum yield (Q_{Eu}^{Eu}). Considering the particular case of the Eu^{3+} ion, in which the magnetic dipole transition $^5D_0 \rightarrow {}^7F_1$ may be taken as an internal reference, the radiative emission coefficients ($A_{0\rightarrow J}$) for the $^5D_0 \rightarrow {}^7F_J$ (J = 2, 4, and 6) transitions may be determined based on Equation 2:

$$A_{0\rightarrow J} = \left(\frac{S_{0\rightarrow J}}{S_{0\rightarrow 1}}\right) A_{0\rightarrow 1} \quad (2)$$

where $A_{0\rightarrow 1}$ is the radiative coefficient assigned to the $^5D_0 \rightarrow {}^7F_1$ transition, which is almost insensible to the chemical environment around the Eu^{3+} ion, while $S_{0\rightarrow 1}$ and $S_{0\rightarrow J}$ are the areas under the emission curves of the $^5D_0 \rightarrow {}^7F_1$ and $^5D_0 \rightarrow {}^7F_J$, respectively (Table S2). From the determined values of $A_{0\rightarrow J}$, the radiative ($A_{rad} = \sum A_{0\rightarrow J}$) and non-radiative ($A_{nrad} = A_{total} - A_{rad}$) rates were calculated. The radiative and total decay rates were used to determine the intrinsic quantum yield Equation 3:

$$Q_{Eu}^{Eu} = \frac{A_{rad}}{A_{rad} + A_{nrad}} = A_{rad} \cdot \tau \quad (3)$$

Further, considering the relationship between $A_{0\rightarrow J}$ and the Judd-Ofelt intensity parameters Ω_λ (λ = 2, 4 and 6) for transitions of the Eu^{3+} ion, these latter were also determined according to Equation 4:

$$\Omega_\lambda = \frac{3\hbar c^3 A_{0\rightarrow\lambda}}{4e^2\omega^3\chi\left\langle {}^7F_\lambda \| U^{(\lambda)} \| {}^5D_0 \right\rangle^2} \quad (4)$$

where ω is the angular frequency of the transition, e is the elementary charge, $\chi = \frac{n\left(n^2+2\right)^2}{9}$ is the Lorentz local field correction and n is the linear index of refraction of the medium (n ≈1.5 for most cases of lanthanide β-diketonate complexes,[22a] $\hbar$ is the reduced Planck's constant, and c is the speed of light. The values for the squared reduced matrix elements $\left\langle {}^7F_\lambda \| U^{(\lambda)} \| {}^5D_0 \right\rangle^2$ are equal to 0.0032 and 0.0023 for λ = 2 and 4, respectively.[22b]

To get a deeper insight into the luminescence sensitization processes in the synthesized compounds, the absolute emission quantum yields (Q_{Eu}^L) were measured upon excitation on the intraligand $S_0 \rightarrow S_1$ transition of the β-diketonate ligands. To determine the Q_{Eu}^L values, the emission and reflectance spectra were carried out for a sample directly excited in the integrating sphere and the integrating sphere without the sample. Based on the spectral results, the quantum yields for solid-state compounds were calculated using the following Equation 5:[22c]

$$Q_{Eu}^L = \frac{E_c - E_a}{L_a - L_c} \quad (5)$$

where E_c is the integrated emissions due to the direct excitation illumination from the integrating sphere. E_a is the integrated emission from an empty integrating sphere. L_a is the integrated excitation profile from the empty integrating sphere (without the sample, only a blank), and L_c is the integrated excitation profile from the sample in the integrating sphere.

As can be seen in Table 3, the experimental intensity parameter Ω_2 values show a significant variation by changing the β-diketonate ligand in the first coordination sphere of the Eu^{3+} ion. The highest and the lowest values were found for the **Eu-4** and **Eu-5** compounds containing tfac and bzac ligands, respectively. It also noted that an almost linear relationship between the Ω_2 and A_{rad} values is obtained, while this trend is not observed for Ω_4, as depicted in Figure S10. This optical result indicates that the $^5D_0 \rightarrow {}^7F_2$ transition dominates the

Research Article
doi.org/10.1002/ejic.202300660

Table 3. Experimental intensity parameters (Ω_2 and Ω_4, in units of 10^{-20} cm^2), decay lifetime (τ in ms), radiative (A_{rad} in s^{-1}) and non-radiative (A_{nrad} in s^{-1}) rates. Q^{Eu}_{Eu} is the intrinsic quantum yield (in %), the ratio between the radiative rate and the total decay rate. Q^{L}_{Eu} is the absolute quantum yield (in %), the ratio between emitted photons per second by the absorbed photons per second by the system. (η_{sens}) Sensitization (in %) by using intrinsic and absolute quantum yields by the relation.

Eu^{3+}-Compound	τ	Ω_2	Ω_4	A_{rad}	A_{nrad}	Q^{Eu}_{Eu}	Q^{L}_{Eu}	η_{sens}
$Eu(tta)_3(dppeO_2)$	0.74	27	6	935	414	69	60	87
$Eu(btf)_3(dppeO_2)$	0.74	25	7	870	489	64	47	73
$Eu_2(dbm)_6(dppeO_2)$	0.48	37	11	1293	806	62	50	81
$Eu(tfac)_3(dppeO_2)$	0.92	20	8	746	343	69	43	62
$Eu(bzac)_3(dppeO_2)$	0.66	20	7	738	779	49	19	39
$Eu_2(fod)_6(dppeO_2)$	0.54	27	6	929	934	50	17	33

luminescent properties of the Eu(β-dik)$_3$(dppeO$_2$) (β-dik: tta, btf, dbm and tfac) and Eu$_2$(fod)$_6$(dppeO$_2$) compounds. Moreover, the observed changes for the Ω_2 values indicate higher azimuthal angular variations in the first coordination sphere following this tendency:[23] **Eu-3** > **Eu-1**~**Eu-6** > **Eu-2** > **Eu-4**~**Eu-5**. In other words, the variation in Ω_2 suggests that changes in the angular arrangement of the first coordination sphere of Eu^{3+} ions are likely influenced more by intermolecular interactions. In addition, the Ω_4 parameter is known to be highly sensitive to the covalent character of the chemical bond between the lanthanide ion and the ligating atom.[24a,b] Therefore, the Ω_4 values indicate that Eu^{3+}–O distances are likely similar across the series, except for the **Eu-3** compound.

The values of A_{rad} for **Eu-1**, **Eu-2**, **Eu-3**, and **Eu-6** compounds are above 870 s^{-1}, while those for the compounds with tfac (**Eu-4**) and bzac (**Eu-5**) present values below 800 s^{-1}. When a more detailed analysis is carried out on the data in Table 3, it is also observed that the non-radiative rate (A_{nrad}) for the **Eu-6** is the highest among the investigated compounds. On the other hand, the A_{nrad} rates are remarkably lower for the **Eu-1**, **Eu-2**, and **Eu-4**, corroborating with the DRS and phosphorescence spectral data that show the absence of excited states capable of acting as efficient channels for depopulation of $^5D_0$ emitting level of the Eu^{3+} ion.

The lowest value of absolute quantum yield $Q^{L}_{Eu} = 17\,\%$ of the **Eu-6** can be mainly explained based on the presence of an LMCT state at low energy that acts as an efficient luminescence quenching pathway.[25] In the case of the **Eu-5** compound with $Q^{L}_{Eu} = 19\,\%$, the phosphorescence data for the analogous Gd-compounds showed that the low-lying triplet state is close to the $^5D_0$ emitting level of the Eu^{3+} ion but slightly below the $^5D_1$ level. Thus, the back energy transfer $^5D_1 \rightarrow T_1$ may be expected, and this should be sufficient to drop the Q^{L}_{Eu} value. For the highest brightening **Eu-1** compound, the values of $Q^{L}_{Eu} = 60\,\%$ reflects an almost ideal combination of a very efficient intramolecular energy transfer ($T_1 \rightarrow {}^5D_1$, $^5D_0$) together with a higher radiative decay and significantly lower non-radiative contribution. The compounds with btf (**Eu-2**) and tfac (**Eu-4**) exhibit intermediate values of the Q^{L}_{Eu} of 47 % and 43 % (Table 3), owing to a decrease in the radiative rate contributions compared to **Eu-1**.

We can estimate the efficiency of sensitization (η_{sens}) by using the ratio between absolute and intrinsic quantum yields.[26] **Eu-1** and **Eu-3** have high-efficiency rates (87 and 81 %), indicating an efficient ligand-to-Eu^{3+} energy transfer. On the other hand, **Eu-5** and **Eu-6** have low sensitization efficiency rates (39 and 33 %), as expected.

Although the radiative rates (A_{rad}) for the investigated compounds are comparable to other highly luminescent systems reported in the literature,[20a] the behavior of the intrinsic quantum yield (Q^{Eu}_{Eu}) values better reflect the most pronounced changes in non-radiative rates (A_{nrad}) (Table 3). For example, the compounds with tta (**Eu-1**), btf (**Eu-2**) and tfac (**Eu-4**) ligands present lower and higher values of A_{nrad} and Q^{Eu}_{Eu}, respectively. While for the other compounds the opposite trend is observed. However, even for the compounds with dbm (**Eu-3**), bzac (**Eu-5**) and fod (**Eu-6**) β-diketonate ligands, the values of Q^{Eu}_{Eu} are still higher than those for the precursor aquo-complexes.[12,27]

The coordinates in the CIE (*Commission Internationale l'Eclairage*) chromaticity diagrams for the investigated compounds in the solid state were determined from the emission spectral data recorded under excitation at intraligand transition at room temperature (Figure 6a). As can see in Table S3, all compounds show very similar values of color coordinates (x,y) located in the red region, reflecting the dominant intensity of the $^5D_0 \rightarrow {}^7F_2$ transition at approximately 612 nm. Just for illustrative purposes, Figure 6b shows the digital camera photographs of the complexes in the solid-state when excited at 365 nm.

In memory of Brian R. Judd, who sadly departed on April 8, 2023, at the age of 92, and in conjunction with C. K. Jørgensen (passed away on January 9, 2001), we would like to pay tribute. Their groundbreaking work in 1964[28] attributed the effects of inhomogeneities in the dielectric surrounding a lanthanide ion to the high variations in intensity parameters, named as "pseudo-quadrupolar mechanism". A decade later, Mason, Peacock, and Stewart published a seminal paper introducing the "dynamic coupling mechanism" in hypersensitive transitions.[29] Remarkably, in 1979, Judd demonstrated that the so-called dynamic coupling mechanism proposed by Manson et al. was formally identical to his mechanism based on an inhomogeneous dielectric in 1964.[30] As a supplement to this narrative, we draw attention to the work of M. Hatanaka and S. Yabushita,[31] emphasizing the necessity of incorporating the dynamic coupling mechanism for a comprehensive explanation

Research Article
doi.org/10.1002/ejic.202300660

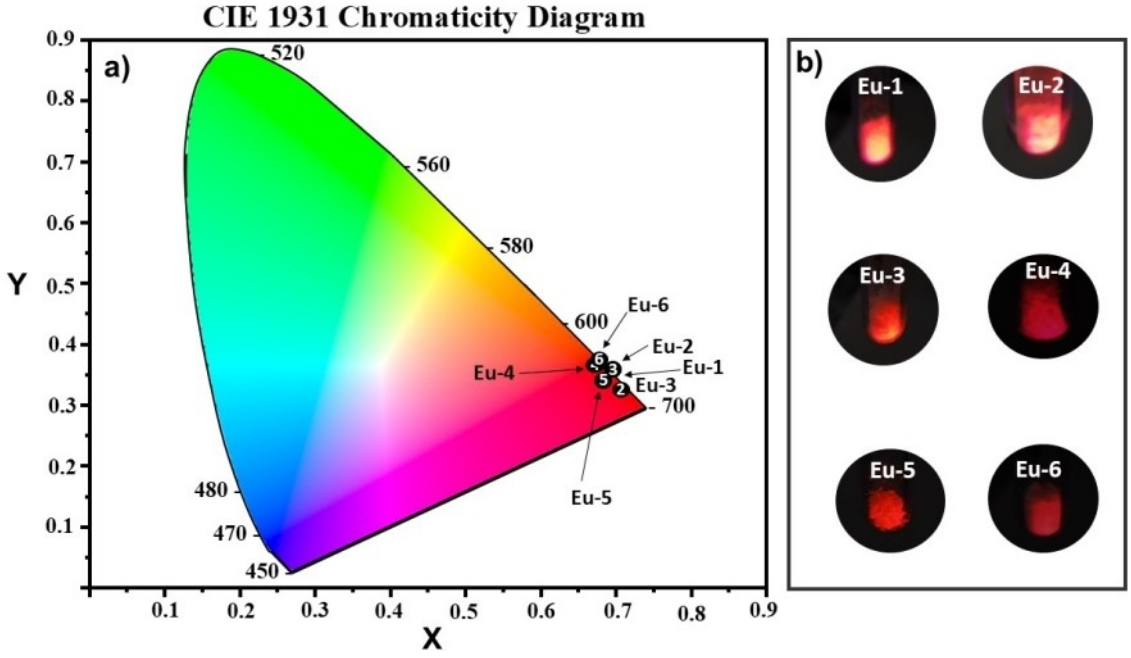

Figure 6. a) CIE diagram containing the color coordinates for the Eu(β-dik)$_3$(dppeO$_2$) (β-dik: tta, btf, bzac and tfac) and Eu$_2$(β-dik)$_6$(dppeO$_2$) (β-dik: dbm and fod) coordination compounds. b) digital camera photographs of the compounds illuminated with a lamp (365 nm) at room temperature.

of hypersensitive transitions. In this continuum of scientific investigation, we pay homage not only to the pioneers but also to new developments and insights that continue to shape the understanding of the intricacies related with lanthanide chemistry.

Conclusions

To sum up, six novel highly luminescent Eu-β-diketonate compounds containing 1,2-Bis(diphenylphosphino)ethane (dppeO$_2$) oxide ancillary ligands were successfully synthesized. The elemental analyses, infrared spectroscopy, and thermal analysis data are consistent with the effective replacement of water molecules in the precursor complexes by the bis(phosphine) oxide ligand. The emission spectral profiles and quantitative properties of the Eu(β-dik)$_3$(dppeO$_2$) (β-dik: tta, btf, bzac and tfac) and Eu$_2$(β-dik)$_6$(dppeO$_2$) (β-dik: dbm and fod) are significantly dependent on the β-diketonates ligands. For the highly brightening **Eu-1** compound, the values of $Q^L_{Eu} = 60\%$ reflects an almost ideal combination of a very efficient intramolecular energy transfer ($T_1 \rightarrow {}^5D_1$, $^5D_0$) together with a higher radiative decay and significantly lower non-radiative rates. The compounds with btf (**Eu-2**) and tfac (**Eu-4**) exhibit Q^L_{Eu} of 47 and 43%, owing to a pronounced decrease of the A_{rad} values when compared with **Eu-1**. The compound with dbm (**Eu-3**) presents both high radiative and non-radiative rates, which may compensate for the gain and losses of the emission process. Compounds **Eu-5** and **Eu-6** showed very low Q^L_{Eu} values equal to 19 and 17%, respectively. In these cases, non-radiative processes are quite operative, but for different reasons. In compound **Eu-5** this behavior can be explained based on the back energy transfer due to the lowest value of the T_1 energy in this series (~18800 cm^{-1}, situated between the $^5D_0$ and $^5D_1$ levels), while for compound **Eu-6**, besides the similarly low value of the T_1, the LMCT state may play an important role in the luminescence quenching.

Finally, all compounds present CIE (x,y) located in the red color region that reflects the prominent behavior of the intraconfigurational $^5D_0 \rightarrow {}^7F_2$ transition. Furthermore, the Eu(β-dik)$_3$(dppeO$_2$) coordination compounds exhibit high luminescence efficiencies.

Experimental Section

Synthesis of the complexes: All complexes were synthesized by reacting the respective aquo-complex with the dppeO$_2$ ligand, using a slightly modified literature procedure.[2b] As an example, the synthesis of the Eu(tta)$_3$(dppeO$_2$) (**Eu-1**) complex is presented.

Under magnetic stirring, a solution of 0.200 g (0.234 mmol) of the Eu(tta)$_3$(H$_2$O)$_2$ complex in ethanol was slowly added dropwise to an ethanolic solution of 1,2-bis(diphenylphosphino)ethane oxide (dppeO$_2$), 0.050 g (0.117 mmol). After approximately 30 minutes, an off-white precipitate was formed. Similar behavior was observed for the syntheses of the complex with the dbm ligand. In the case of the complexes with the btf (**Ln-2**), tfac (**Ln-4**), bzac (**Ln-5**), and fod (**Ln-6**) ligands, the precipitation occurs after the partial evaporation of the solvent. Finally, the precipitate in the powder form was filtered, washed with several portions of cold ethanol, and dried under reduced pressure. Despite exhaustive attempts, no single crystals suitable for X-ray diffraction were obtained. For synthetic details of the Gd-based analogs complexes, see the Supporting Information. The experimental and calculated elemental analyzes

(CHN) and the infrared data are presented below (for relative transmittance s: strong, m: medium, and w: weak):

$Eu(tta)_3(dppeO_2)$ (**Eu-1**) Yield: 150.10 mg (70%). FTIR (in KBr/cm^{-1}): 3061 (w), 2912 (w), 1608 (s), 1537 (s), 1500 (m), 1413 (s), 1300(s), 1186(s), 1165 (s), 1139 (s) 933 (m), 858 (m), 783 (m); 694 (m), 642(m) 578(m), 532(m). calcd: C, 48.20; H, 2.91; Eu, 12.20%, found: C, 48.81; H, 2.65; Eu, 12.41%.

$Eu(btf)_3(dppeO_2)$ (**Eu-2**) Yield: 210.70 mg (70%). FTIR (in KBr/cm^{-1}): 3059 (w), 2972 (m), 1614 (s), 1577 (m), 1537 (m), 1473 (m), 1438 (m), 1288 (s), 1163 (s), 1124 (s) 962 (w), 763 (m), 729 (m), 694 (w); 630 (w), 532 (m). calcd: C, 54.00; H, 3.45; Eu, 15.01%, found: C, 54.22; H, 3.32; Eu, 15.79%.

$Eu_2(dbm)_6(dppeO_2)$ (**Eu-3**) Yield: 255.70 mg (80%). FTIR (in KBr/cm^{-1}): 3057 (w), 2906 (w), 1598 (s), 1552 (s), 1516 (S), 1456 (s), 1415(s), 1307(m), 1172 (s), 1164 (m), 1022(m), 727 (s), 690 (m), 607 (m); 694 (m), 532(m),. calcd: C, 67.12; H, 4.47; Eu, 14.66%, found: C, 67.19; H, 4.52; Eu, 14.84%.

$Eu(tfac)_3(dppeO_2)$ (**Eu-4**) Yield: 170.70 mg (63%). FTIR (in KBr/cm^{-1}): 3061 (w), 2920 (m), 1629 (s), 1528 (s), 1491 (s), 1291 (s), 1171(s), 1134 (s), 851 (w), 733 (m), 693 (w), 558 (w); 532 (s). calcd: C, 47.28; H, 3.48; Eu, 14.59%, found: C, 47.35; H, 3.41; Eu, 14.78%.

$[Eu(bzac)_3(dppeO_2)]_n$ (**Eu-5**) Yield: 190.35 mg (65%). FTIR (in KBr/cm^{-1}): 3055 (w), 2910 (w), 1600 (s), 1570 (s), 1516 (s), 1458 (s), 1409(s), 1271(m), 1170 (s), 1120 (m) 1101 (m), 987 (s), 839 (m), 727 (s); 692 (s), 530(s) 503 (m). calcd: C, 63.10; H, 4.82; Eu, 14.26%, found: C, 62.98; H, 4.87; Eu, 14.19%.

$Eu_2(fod)_6(dppeO_2)$ (**Eu-6**) Yield: 175.90 mg (63%). FTIR (in KBr/cm^{-1}): 3066 (w), 2972 (m), 1622 (s), 1508 (s), 1465 (m), 1346 (s), 1226(s), 1186(s), 1165 (s), 1120 (s) 962 (w), 910 (m), 833 (w), 794 (w); 744 (m), 694 (w) 536 (m). calcd: C, 41.23; H, 3.56; Eu, 12.13%, found: C, 41.30; H, 3.41; Eu, 11.78%.

Materials and methods: All experimental procedures were performed using analytical grade reagents. The chemicals: Ethanol (C_2H_6O Tedia, 99.3%), methanol (CH_4O Tedia, 99.8%), chloridric acid (HCl Alfa Aesar 28%), 1,2-Bis(diphenylphosphino)ethane ($C_{26}H_{28}P_2$ Aldrich 99%), thenoyltrifluoroacetone (tta: $C_8H_5F_3O_2S$, Aldrich 99%), 4,4,4-trifluoro-1-phenyl-1,3-butanedione (btf: $C_{10}H_7O_2F_3$ Aldrich 99%), dibenzoylmethane (dbm: $C_{15}H_{12}O_2$ Aldrich 98%), trifluoroacetylacetone (tfac: $C_5H_2O_2F_6$ Aldrich 98%), 1-phenyl-1,3-butanedione (bzac: $C_{10}H_{10}O_2$ Aldrich 99%), 2,2-dimethyl-6,6,7,7,8,8,8-heptafluoro-3,5-octanedione (fod: $C_{10}H_{11}O_2F_7$ Aldrich 99%), europium oxide (Eu_2O_3 Aldrich 99.999%) and gadolinium oxide (Gd_2O_3 Alfa Aesar 99.999%). The lanthanide chloride, $LnCl_3.6H_2O$, (Ln: Eu and Gd), were obtained by reaction between the respective lanthanide oxide Ln_2O_3 and concentrated chloridric acid according to the literature.[32] The complexes of general formula $Ln(\beta\text{-dik})_3(H_2O)_2$ and $Ln(dbm)_3(H_2O)$ complexes (Ln: Eu^{3+} and Gd^{3+} while β-dik: tta, btf, dbm, tfac, bzac and fod) were synthesized according to the procedure reported by Teotonio and co-workers.[12] The 1,2-bis(diphenylphosphino)ethane oxide ($dppeO_2$) was synthesized by reacting 1,2-bis(diphenylphosphino)ethane (dppe) with hydrogen peroxide (H_2O_2).

The Eu^{3+} and Gd^{3+} contents present in the coordination were determined from complexometric titration using EDTA as titrating and xylenol orange as an indicator.[2b] Elemental analyses of C, H and N were performed on a 2400 CHNS analyzer manufactured by PerkinElmer. FTIR spectra of compounds were carried out in the range of 400–4000 cm^{-1} on a Shimadzu FTIR spectrophotometer, model IRPrestige-21, using a KBr pellet and a 4 cm^{-1} spectral resolution. The thermogravimetric analyses were performed in the temperature range from 25 to 900 °C, employing a Shimadzu DTG-60 equipment under a dynamic nitrogen atmosphere and a heating rate of 50 mL min^{-1} and 10 °C min^{-1}, respectively. Diffuse reflectance spectra (DRS) measurements were carried out in the spectral range from 190 to 600 nm on a UV-VIS spectrophotometer Shimadzu UV2600i using an integrating coated with $BaSO_4$. The stead-state luminescence spectra (excitation and emission) for the solid-state samples at room temperature (~300 K) were recorded on the front-face 22.5° angle on a HORIBA Fluorolog-3 (FL22) spectrofluorometer. In this case, a 450 W xenon lamp as an excitation source and the R928P PMT photomultiplier as a detector. The time-resolved emission spectra of the Gd-compounds and the luminescence decay curves were recorded using a 50 W pulsed xenon lamp and SPEX 1934D phosphorimeter coupled to the same spectrofluorometer. To determine the absolute quantum yield values of the complexes in the solid-state phase a HORIBA Quanta-ϕ integrating sphere was used, which was coupled to the Fluorolog-3 spectrofluorimeter via fiber-optic cables and F-3000 Fiber-Optic Adapter.

Powder X-ray diffraction: The Powder X-ray diffraction pattern (PXRD) for $[Eu(bzac)_3(dppeO_2)]_\infty$ coordination polymer was recorded using a Shimadzu LabX XRD-6000 diffractometer with a monochromated Cu–Kα ($\lambda = 1.5418$ Å) radiation. The experimental conditions were the following: Speed equal to 1.2 s/step and step size of 0.02° (2θ) at room temperature (300 K) in the range of $2\theta = 5–50°$. The simulated PXRD pattern was obtained from single-crystal diffraction data using CCDC Mercury 3.0 program.

Single Crystal X-ray Diffraction: The crystal collection parameters and structural refinement data for the compound $[Eu(bzac)_3(dppeO_2)]_\infty$ are given in Table S4.

Deposition Number(s) 2304127 (for **Eu-5**) contain(s) the supplementary crystallographic data for this paper. These data are provided free of charge by the joint Cambridge Crystallographic Data Centre and Fachinformationszentrum Karlsruhe Access Structures service.

A suitable single crystal of the $[Eu(bzac)_3(dppeO_2)]$n coordination polymer for X-ray diffraction was obtained from the crystallization of the titled compound from an ethanol solution. The diffraction data were collected on a Bruker-AXS Kappa Apex II Duo equipment using Mo Ka radiation ($\lambda = 0.71073$ Å) from an IμS microsource, filtered by X-ray optics multilayer mirrors. The APEX 3 suite of programs and the multi-scan method with SADABS were used to reduce and correct the obtained raw data for analysis purposes. Finally, the chemical structure solution was performed employing direct methods using SHELXT software, while the final refinement was performed with full matrix least squares in F2 using SHELXL-2019. The ORTEP-3[33a] and SHELXL-2019[33b] software from the WinGX package were used.

Support Information

The authors cited additional references in the Supporting Information.[34–36]

Author Contributions

The manuscript was written with the contributions of all authors. All authors have approved the final version of the manuscript.

P. R. S. Silva: Conceptualization, Methodology, Investigation, Formal Analysis, Data Curation, Validation, Visualization, Writing – Original Draft, Writing – Review & Editing. **A. A. S. S. Jesus**: Conceptualization, Methodology, Investigation, Formal

Analysis, Data Curation. **W. B. Lima**: Conceptualization, Methodology, Investigation, Formal Analysis, Data Curation. **J. G. Arruda**: Methodology, Investigation, Formal Analysis, Data Curation. **I. F. Costa**: Formal Analysis, Data Curation, Validation, Visualization, Writing – Review & Editing. **W. M. Faustino**: Resources, Supervision, Writing – review & editing. **M. C. F. C. Felinto**: Data curation, Investigation, Writing – original draft. **J. R. Sabino**: Data curation, Investigation, Writing – original draft. **H. F. Brito**: Data curation, Investigation, Writing – original draft. **R. T. Moura Jr.**: Software, Validation, Writing – Review & Editing. **A. N. Carneiro Neto**: Software, Validation, Visualization, Data curation, Investigation, Writing – original draft, Writing – Review & Editing. **O. L. Malta**: Data curation, Investigation, Writing – original draft. **H. Terraschke**: Investigation, Methodology, Writing – Review & Editing. **E. E. S. Teotonio**: Conceptualization, Funding acquisition, Investigation, Methodology, Project administration, Resources, Supervision, Writing – original draft, Writing – review & editing.

Acknowledgements

This work was funded by the Universidade Federal da Paraíba (PRODUTIVIDADE UFPB 03/2020, PVA13345-2020). The authors also thank Conselho Nacional de Desenvolvimento Científico e Tecnológico (CNPQ: 313195/2018-8) and Coordenação de Aperfeiçoamento de Pessoal de Nível Superior (CAPES/DAAD: 88887.647236/2021-00 and 88887.371434/2019-00) and Fundação de Amparo à Pesquisa do Estado de São Paulo (FAPESP: 2021/08111-2). This work was developed within the scope of the project CICECO- Aveiro Institute of Materials, UIDB/50011/2020, UIDP/50011/2020 & LA/P/0006/2020 and Shape of Water (PTDC/NAN-PRO/3881/2020) financed by Portuguese funds through theFCT/MEC (PIDDAC).

Conflict of Interests

There are no conflicts to declare.

Data Availability Statement

The data that support the findings of this study are available from the corresponding author upon reasonable request.

Keywords: bisphosphine oxides · Europium · β-diketonate · luminescence quantum yield · photoluminescence properties

[1] S. I. Weissman, *J. Chem. Phys.* **1942**, *10*, 214–217.
[2] a) H. Wang, H. Li, Y. Zhang, X. Chen, *J. Mol. Struct.* **2022**, *1270*, 2045–2052; b) F. A. Silva, H. A. Nascimento, D. K. S. Pereira, E. E. S. Teotonio, H. F. Brito, M. C. F. C. Felinto, J. G. P. Espínola, G. F. Sá, W. M. Faustino, *J. Braz. Chem. Soc.* **2013**, *24*, 601–608.
[3] a) J. F. C. B. Ramalho, A. N. Carneiro-Neto, L. D. Carlos, P. S. André, R. A. S. Ferreira, *Handbook on the Physics and Chemistry of Rare Earths*. Eds.; Elsevier B. V., **2022**, p. 31; b) Y. Ning, S. Zhao, D. Song, B. Qiao, Z. Xu, Y. Zhou, J. Chen, W. Swelm, A. Al-Ghamdi, *ACS Polym.* **2022**, *14*, 662–665; c) M. Fang, A. N. Carneiro-Neto, L. Fu, R. A. S. Ferreira, V. de Zea-Bermudez, L. D. Carlos, *Adv. Mater. Technol.* **2022**, *7*, 2100727; d) E. V. Salerno, A. N. Carneiro-Neto, S. V. Eliseeva, M. A. Hernández-Rodríguez, J. C. Lutter, T. Lathion, J. W. Kampf, S. Petoud, L. D. Carlos, V. L. Pecoraro, *J. Am. Chem. Soc.* **2022**, *144*, 18259–18271; e) X. Ou, X. Qin, B. Huang, J. Zan, Q. Wu, Z. Hong, L. Xie, H. Bian, Z. Yi, X. Chen, Y. Wu, X. Song, J. Li, Q. Chen, H. Yang, X. Liu, *Nature* **2021**, *590*, 410–415; f) R. Piñol, J. Zeler, C. D. S. Brites, Y. Gu, P. Téllez, A. N. Carneiro-Neto, T. E. Da Silva, R. Moreno-Loshuertos, P. Fernandez-Silva, A. I. Gallego, L. Martinez-Lostao, A. Martínez, L. D. Carlos, *Nano Lett.* **2022**, *20*, 6466–6472; g) A. Bednarkiewicz, J. Drabik, K. Trejgis, D. Jaque, E. Ximendes, L. Marciniak, *Appl Phys Rev.* **2021**, *8*, 11317.
[4] O. L. Malta, F. R. Gonçalves E Silva, *Spectrochim. Acta Part A* **1998**, *54*, 1593–1599.
[5] W. M. Faustino, O. L. Malta, G. F. De Sá, *J. Chem. Phys.* **2005**, *122*, 215–219.
[6] a) W. M. Faustino, O. L. Malta, G. F. De Sá, *J. Chem. Phys.* **2006**, *122*, 150–157; b) W. M. Faustino, O. L. Malta, E. E. S. Teotonio, H. F. Brito, A. M. Simas, G. F. de Sá, *J. Phys. Chem. A* **2006**, *110*, 2510–2516.
[7] T. Miyakawat, D. L. Dextkrt, *Phys. Rev. B* **1970**, *1*, 2961–2969.
[8] K. Binnemans, *Coord. Chem. Rev.* **2015**, *295*, 1–45.
[9] a) H. Han, B. Wang, L. Yu, C. Dai, X. Wang, Y. Wang, *Infrared Phys. Technol.* **2022**, *125*, 150–158; b) H. Liu, C. Deng, Q. Chen, X. Shen, *Polyhedron.* **2016**, *117*, 309–317.
[10] a) E. E. S. Teotonio, H. F. Brito, M. C. F. C. Felinto, C. A. Kodaira, O. L. Malta, *J. Coord. Chem.* **2003**, *56*, 913–921; b) Y. C. Miranda, L. L. A. L. Pereira, J. H. P. Barbosa, H. F. Brito, M. C. F. C. Felinto, O. L. Malta, W. M. Faustino, E. E. S. Teotonio, *Eur. J. Inorg. Chem.* **2015**, *2015*, 3019–3027.
[11] A. W. G. Platt, *Coord. Chem. Rev.* **2017**, *340*, 62–78.
[12] J. L. Moura, I. F. Costa, P. R. S. Santos, I. F. Silva, R. T. Moura, A. N. Carneiro Neto, W. M. Faustino, H. F. Brito, J. R. Sabino, E. E. S. Teotonio, *Inorg. Chem.* **2022**, *61*, 13510–13524.
[13] a) Y. Kitagawa, M. Kumagai, P. P. Ferreira da Rosa, K. Fushimi, Y. Hasegawa, *Chem. Eur. J.* **2021**, *27*, 264–269; b) Y. Kitagawa, A. Naito, K. Aikawa, K. Shima, S. Shoji, K. Fushimi, Y. Hasegawa, *Chem. Eur. J.* **2022**, *28*, e2021104401; c) Y. Kitagawa, P. P. Ferreira da Rosa, Y. Hasegawa, *Dalton Trans.* **2021**, *50*, 14978–14984; d) M. Tsurui, Y. Kitagawa, K. Fushimi, M. Gon, K. Tanaka, Y. Hasegawa, *Dalton Trans.* **2020**, *49*, 5352–5361; e) M. Yamamoto, T. Nakanishi, Y. Kitagawa, T. Seki, H. Ito, K. Fushimi, Y. Hasegawa, *Bull. Chem. Soc. Jpn.* **2018**, *91*, 6–11.
[14] a) P. P. Ferreira da Rosa, Y. Kitagawa, Y. Hasegawa, *Coord. Chem. Rev.* **2020**, *406*, 218–221; b) D. A. Lima, A. G. Bispo-Jr, D. A. Galico, S. F. N. Coelho, J. H. Araujo Neto, J. A. Ellena, L. Petiote, I. O. Mazali, F. A. Sigoli, *Inorg. Chem.* **2023**, *17*, 6808–6816; c) K. Miyata, Y. Hasegawa, Y. Kuramochi, T. Nakagawa, T. Yokoo, T. Kawai, *Eur. J. Inorg. Chem.* **2009**, *32*, 4777–4785; d) Y. Hasegawa, *Bull. Chem. Soc. Jpn.* **2011**, *84*, 148–154; e) Y. Hasegawa, Y. Miura, Y. Kitagawa, S. Wada, T. Nakanishi, K. Fushimi, T. Seki, H. Ito, T. Iwasa, T. Taketsugu, M. Gon, K. Tanaka, Y. Chujo, S. Hattori, M. Karasawa, K. Ishii, *Chem. Commun.* **2018**, *54*, 10695–10697.
[15] H. B. Xu, J. Wang, X. L. Chen, P. Xu, K. T. Xiong, D. Bin Guan, J. G. Deng, Z. H. Deng, M. Kurmoo, M. H. Zeng, *Dalton Trans.* **2018**, *47*, 6908–6916.
[16] H. Yan, Zi-Wei Che, Wen-Bin Sun, *New J. Chem.* **2023**, *47*, 140–146.
[17] E. E. S. Teotonio, J. G. P. Espínola, H. F. Brito, O. L. Malta, S. F. Oliveira, D. L. A. De Faria, C. M. S. Izumi, *Polyhedron.* **2002**, *21*, 1837–1844.
[18] W. M. Faustino, O. L. Malta, G. F. de Sá, *Chem. Phys. Lett.* **2006**, *429*, 595–599.
[19] P. R. S. Santos, D. K. S. Pereira, I. F. Costa, I. F. Silva, H. F. Brito, W. M. Faustino, A. N. Carneiro Neto, R. T. Moura, M. H. Araujo, R. Diniz, O. L. Malta, E. E. S. Teotonio, *J. Lumin.* **2020**, *226*, 17455.
[20] a) A. N. Carneiro Neto, E. E. S. Teotonio, G. F. de Sá, H. F. Brito, J. Legendziewicz, L. D. Carlos, M. C. F. C. Felinto, P. Gawryszewska, R. T. Moura, R. L. Longo, W. M. Faustino, O. L. Malta, *Handbook on the Physics and Chemistry of Rare Earths*, **2019**, 162; b) C. K. Jorgensen, B. R. Judd, *Mol. Phys.* **1964**, *8*, 281–290.
[21] K. Binnemans, *Coord. Chem. Rev.* **2015**, *295*, 1–45.
[22] a) K. P. Zhuravlev, V. I. Tsaryuk, V. A. Kudryashova, *J Fluor Chem.* **2018**, *212*, 137–143; b) W. T. Carnall, H. M. Crosswhite, *Inorg. Chem.* **1966**, *5*, 1466; c) Quanta-φ F-3029 Integrating Sphere Operation Manual rev. C, **2010**. http://www.HORIBA.com/scientific.
[23] I. F. Costa, L. Blois, A. N. Carneiro-Neto, E. E. S. Teotonio, H. F. Brito, L. D. Carlos, M. C. F. C. Felinto, R. T. Moura Jr, R. L. Longo, W. M. Faustino, O. L. Malta, *Reinterpreting the Judd-Ofelt parameters based on recente theoretical advances*, De Gruyter, Berlin, **2023**.
[24] a) N. S. Kariaka, V. A. Trush, Viktoriya. V. Dyakonenko, S. V. Shishkina, S. S. Smola, N. V. Rusakova, T. Y. Sliva, P. Gawryszewska, A. N. Carneir-

Research Article
doi.org/10.1002/ejic.202300660

o Neto, O. L. Malta, V. M. Amirkhanov, *ChemPhysChem* **2022**, *23*, E20220012; b) M. Hatanaka, S. Yabushita, *Theor. Chem. Acc.* **2014**, *133*, 1517.
[25] Y. An, G. E. Schramm, M. T. Berry, *J. Lumin.* **2002**, *97*, 7–12.
[26] A. N. Carneiro Neto, R. T. Moura, L. D. Carlos, O. L. Malta, M. Sanadar, A. Melchior, E. Kraka, S. Ruggieri, M. Bettinelli, F. Piccinelli, *Inorg. Chem.* **2022**, *61*, 16333–16346.
[27] G. B. V. Lima, J. C. Bueno, A. F. da Silva, A. N. Carneiro Neto, R. T. Moura, E. E. S. Teotonio, O. L. Malta, W. M. Faustino, *J. Lumin.* **2020**, *219*, 2019–2025.
[28] B. R. Judd, K. Jorgensen, *Mol. Phys.* **1964**, *8*, 281–290.
[29] B. R. Judd, *J. Chem. Phys.* **1979**, *70*, 4830–4833.
[30] S. F. Mason, R. D. Peacock, B. Stewart, *Chem. Phys. Lett.* **1974**, *29*, 149–153.
[31] M. Hatanaka, S. Yabushita, *Theor. Chem. Acc.* **2014**, *133*, 1517(1–15).
[32] J.-C. G. Bünzli, *Coord. Chem. Rev.* **2015**, *47*, 293–294.
[33] a) L. J. Farrugia, *J. Appl. Crystallogr.* **1997**, *30*, 565–565; b) G. M. Sheldrick, *Acta Crystallogr. Sect. A* **2008**, *64*, 112–122.
[34] E. E. S. Teotonio, G. M. Fett, H. F. Brito, W. M. Faustino, G. F. de Sá, M. C. F. C. Felinto, R. H. A. Santos, *J. Lumin.* **2008**, *128*, 190–198.
[35] L. Blois, A. N. C. Neto, R. L. Longo, I. F. Costa, T. B. Paolini, H. F. Brito, O. L. Malta, *Opt. Spectrosc.* **2020**, *130*, 10–17.
[36] J. Mooney, P. Kambhampati, *Phys. Chem. Lett.* **2013**, *4*, 3316–3318.

Manuscript received: October 30, 2023
Revised manuscript received: November 27, 2023
Accepted manuscript online: November 29, 2023
Version of record online: December 19, 2023